Appl. Math. J. Chinese Univ.
2024, 39(1): 34-46

Insight into the dynamics of non-Newtonian Carreau fluid when viscous dissipation, entropy generation, convective heating and diffusion are significant

ZHOU Shuang-shuang[1] Muhammad Ijaz Khan[2,*]
Sami Ullah Khan[3] Sumaira Qayyum[4]

Abstract. The investigation endorsed the convective flow of Carreau nanofluid over a stretched surface in presence of entropy generation optimization. The novel dynamic of viscous dissipation is utilized to analyze the thermal mechanism of magnetized flow. The convective boundary assumptions are directed in order to examine the heat and mass transportation of nanofluid. The thermal concept of thermophoresis and Brownian movements has been re-called with the help of Buongiorno model. The problem formulated in dimensionless form is solved by NDSolve MATHEMATICA. The graphical analysis for parameters governed by the problem is performed with physical applications. The affiliation of entropy generation and Bejan number for different parameters is inspected in detail. The numerical data for illustrating skin friction, heat and mass transfer rate is also reported. The motion of the fluid is highest for the viscosity ratio parameter. The temperature of the fluid rises via thermal Biot number. Entropy generation rises for greater Brinkman number and diffusion parameter.

§1 Introduction

The improved energy transportation is the main requirement in many industrial as well as engineering processes to achieve maximum manufacturing achievements. Based on some traditional methods, the improvement in heat transfer is not sufficient to attain the desirable task. The addition of nanoparticles in the uniform base liquids is the most optimized way to improve the thermal efficiency and meet the energy requirements. The modification in thermal characteristics of base liquids is suggested with the addition of nano-sized metallic

Received: 2018-12-07. Revised: 2021-04-01.
MR Subject Classification: 76R05, 80A20, 76Wxx, 35Q30.
Keywords: heat generation, surface reaction, CNTs based nanofluid, stretching/shrinking sheet, thermal radiation.
Digital Object Identifier(DOI): https://doi.org/10.1007/s11766-024-3682-y.
*Corresponding author.

particles in the base materials like ethylene alcohol, water, oil etc. The nano-materials like carbides, metals, and carbon nano-tubes are characterized as the most efficient source of energy with dynamic thermal properties. The applications of nanofluids account in various thermal systems, air conditioning, power generation, extrusion processes, power plants, condensers, engineering devices, heating applications evaporators etc. The experimental investigation of these nanofluid properties was originally directed by Choi [1]. The theoretical analysis which deals with the Brownian and thermophoretic slip mechanism was worked out by Buongiorno [2]. Turkyilmazoglu [3] presented the fully developed nanofluid theoretical analysis accounted in the concentric annuli with single and dual phase nanofluid models. Souayeh et al. [4] presented research on the nanofluid properties of ferromagnetic and titanium nanoparticles in presence of slip mechanism and radiative assessment. The various flow pattern on base fluids along with nanoparticles of tinny size with the mechanism of meta-analysis was reported numerically by Wakif et al. [5]. According to this interesting investigation, the meta-analysis on the effects of thermophoresis shows that different responses to the force of a temperature gradient are sufficient enough to enhance the temperature distribution due to an increase in thermophoresis. Hajizadeh et al. [6] incorporated the damped constraints thermal flux in nanofluid flow which is placed between the surfaces of two plates. Nisar et al. [7] identified the peristaltic transport of Eyring-Powell nanofluid with external applications of activation energy. The theoretical analysis which reports the thermal efficiency of cobalt ferroparticles in the wavy configuration has been worked out by Mustafa and co-researchers [8]. Chu et al. [9] numerically explored the thermal enhancement of nanofluid with Eyring Powell non-Newtonian material by employing interesting pseudo-spectral collocation technique. The accelerated movement of Maxwell nanofluid with an effective influence of thermal radiation and motile microorganisms was analytically done by Chu et al. [10]. Kumar et al. [11] presented an extended analysis for couple stress nanofluid problem in Ohmic dissipation. Oke et al. [12] examined the significance of Coriolis force and heat source/sink in 47 nm alumina-water nanofluids confined by rotating surface.

The heat transfer mechanism and different thermal extrusion processes are associated with the theories of thermodynamics. Following the first thermodynamics law, energy can be renovated in different systems without any loss or decrement. However, justification of irreversibilities (entropy process) cannot be justified with the aim of first thermodynamics low. The irreversibility accounted for within the system is termed entropy generation. The second thermodynamics theory successfully intends the consumption of energy and subsequently reduces the decrement in the transportation of energy. The decrement in the energy is helpful to improve the efficiency performance of heat transfer. The entropy generation is referred to as the major problem in the era of thermodynamics. The efficiency of various devices and machines needs to optimize the entropy generation. Some major contribution on the topic of entropy generation is suggested by many researchers. For example, Kumar et al. [13] examined the transient entropy generation assessment for the flow of Jeffrey nanofluid confined by a vertical flat surface. Shukla et al. [14] simulated the magnetized flow of nanofluid in presence of entropy generation phenomenon. Salimi et al. [15] utilized the entropy generation pattern while examining the 3-D flow of nanofluid encountered by porous jet. The chemical reactive flow of nanofluid in presence of entropy gen-

eration assessment has been visualized by Khan et al. [16]. Chu et al. [17] analyzed the aspects of entropy generation in modified double diffusion flow of viscoelastic nanofluid having variable thermal conductivity. The radiative flow of Casson nanofluid along with entropy generation inspection was analytically presented in the investigation of Khan et al. [18]. Seyyedi et al. [19] signified the entropy generation importance in L-shaped enclosure subject to the magnetic force. Kumar et al. [20] analyzed the natural convection dissipative flow of nanofluid along with entropy production in viscoelastic fluid. The work continued by Khan et al. [21] deals with the Jeffrey nanofluid flow with entropy generation affiliation confined by a curved surface.

The developed interest of scientists towards non-Newtonian fluids is due to their un-predicted and multidisciplinary behavior. The non-Newtonian fluids obey fascinating significances in the chemical industries, food sciences, mechanical processes and many pharmaceutical industries. Due to highly complicated behavior and nature, some exclusive types of non-Newtonian materials are claimed in the existing literature. The Carreau fluid model reflects the complicated rheology of nonlinear materials like polymer solutions successfully. At any value of shear rate, the viscosity of shear thickening is more than that of shear-thinning but there will be a particular time whereby the viscosity of shear thickening and shear thinning will be the same [21]. Carreau [22] intended the basic work on the flow of Carreau fluid for which the Cauchy stress tensor is given by:

$$\tau = -p\mathbf{I} + \mu(\dot{\gamma})\mathbf{A}_1 \tag{1}$$

with [22]

$$\mu(\dot{\gamma}) = \mu_\infty 1 + (\mu_0 - \mu_\infty)\left[1 + (\beta_1\dot{\gamma})\right]^{\frac{n-1}{2}} \tag{2}$$

With pressure p, identity tensor $\mathbf{I}$, zero viscosity (μ_0), infinite viscosity (μ_∞), material constant β_1 and $\mathbf{A}_1$ is first Rivlin-Erickson tensor. For shear rate.

$$\dot{\gamma} = \sqrt{\frac{1}{2}\dot{t}\,(\mathbf{A}_1^2)} \tag{3}$$

With concept of $\mu_0 \geq \mu_\infty$ and μ_∞ vanishes. Thus Eq (1) becomes [22].

$$\tau = -p\mathbf{I} + \mu_0\left[1 + (\beta_1\dot{\gamma})^2\right]^{\frac{n-1}{2}}\mathbf{A}_1. \tag{4}$$

This investigation analyzes the optimized flow of a non-Newtonian nanofluid in presence of viscous dissipation, magnetic force and entropy generation assessment. The classical rheological dynamic of the non-Newtonian model is assessed by using the famous Carreau nanofluid model [23-26]. Consequence to the novel aim and motivations, the current analysis accesses answers to the following research questions:

- How thermal characteristics of Carreau non-Newtonian fluid are improved with utilization of nanofluids?
- What is the significance of the entropy generation phenomenon in the flow of Carreau nanofluid?
- How heat and mass transportation process influenced with impact of magnetic force and viscous dissipation?
- What is the physical significance of entropy generation and Bejan number?

- How is combined heat and mass transportation process enhanced by using the convective boundary conditions?

§2 Flow formulation

The incompressible and two-dimensional flow Carreau nanofluid is assumed over a stretched surface which linearly moves with the velocity $u = ax$. The cartesian system is endorsed with an explanation of velocity components u and v. The magnetic force impact is directed vertically with strength B_0. The assumptions of low Reynolds number is followed to neglect the role of induced magnetic force. Let nanofluid temperature (T) and concentration (C) are assumed to be uniform. The viscous dissipation relations are flowed to modify the heat equation. The free stream concept of nanofluid temperature and concentration is symbolized with T_∞ and C_∞, respectively. The problem is modeled in the following equation [22-25]:

$$\frac{\partial v}{\partial y} + \frac{\partial u}{\partial x} = 0 \tag{5}$$

$$u\frac{\partial u}{\partial x} + v\frac{\partial u}{\partial y} = v\frac{\partial^2 u}{\partial y^2}\left[\beta_1 + (1-\beta_1)\left\{1 + \Gamma^2\left(\frac{\partial u}{\partial y}\right)^2\right\}^{\frac{n-1}{2}}\right] + \left(\frac{\partial u}{\partial y}\right)^2\left\{1 + \Gamma^2\left(\frac{\partial u}{\partial y}\right)^2\right\}^{\frac{n-3}{2}} + g\left[\gamma_1\left(T - T_\infty\right) + \gamma_2\left(C - C_\infty\right)\right] + v(n-1)(1-\beta)\Gamma^2\left(\frac{\partial^2 u}{\partial y^2}\right) - \frac{\sigma B_0^2}{\rho}(u) \tag{6}$$

$$u\frac{\partial T}{\partial x} + v\frac{\partial T}{\partial y} = \alpha_{nf}\frac{\partial^2 T}{\partial y^2} + \tau\left\{\frac{D_B}{C_0}\frac{\partial T}{\partial y}\frac{\partial C}{\partial y} + \frac{D_T}{T_\infty}\frac{\partial T}{\partial y}\frac{\partial T}{\partial y}\right\} + \frac{v}{c_p}\left[\beta_1 + (1-\beta_1)\left\{1 + \Gamma^2\left(\frac{\partial u}{\partial y}\right)^2\right\}^{\frac{n-1}{2}}\right]\left(\frac{\partial u}{\partial y}\right)^2 \tag{7}$$

$$u\frac{\partial C}{\partial x} + v\frac{\partial C}{\partial y} = D_B\frac{\partial^2 C}{\partial y^2} + \frac{C_0 D_T}{T_\infty}\frac{\partial^2 T}{\partial y^2} \tag{8}$$

With material parameter Γ, C_0 is reference concentration, electrical conductivity σ, density ρ, nanoparticles to effective heat capacity ratio τ, thermophoretic constant D_τ, Brownian motion D_B, gravity g, thermal conductivity k and power law index n.

$$u = ax, v = 0, -k\frac{\partial T}{\partial y} = h_f\left(T_f - T\right), D_B\frac{\partial C}{\partial y} = h_g\left(C_f - C\right) \text{ at } y = 0. \tag{9}$$

$$u \to 0, T \to T_\infty, C \to C_\infty \text{ at } y \to \infty \tag{10}$$

In order to obtain similarity solution, the variables suggested by Hayat et al. [23], Malik and Salahuddin [24] was considered as:

$$u = axf'(\eta), v = -\sqrt{a\nu}f(\eta), \eta = \sqrt{\frac{a}{v}}y, \theta(\eta) = \frac{T - T_\infty}{T_f - T_\infty}, \phi(\eta) = \frac{C - C_\infty}{C_f - C_\infty} \tag{11}$$

In view of above variables, the problem in dimensionless form is:

$$\beta_1 f''' + (1-\beta_1)\left(1 + n(We)^2\right)\left(f''\right)^2 f''' + \frac{n-3}{2}(We)^2\left(f''\right)^2 f''' + \tag{12}$$

$$n\left(\frac{n-3}{2}\right)(We)^4\left(f''\right)^4 f''' + ff'' - \left(f'\right)^2 - Ha^2 f' + \lambda^*\theta + \lambda^*\Omega_1\phi = 0 \tag{13}$$

$$\frac{1}{\Pr}\theta'' + f\theta + Nb\theta\phi' + Nt(\theta)^2 + Ec\left(\beta f''^2 + (1-\beta)\left[f'^2 + (We)^2\left(\frac{n-1}{2}\right)f'^4\right]\right) = 0 \tag{14}$$

$$\phi'' + \left(\frac{Nt}{Nb}\right)\theta'' + Scf'\phi = 0 \tag{15}$$

with boundary conditions

$$\begin{aligned} f(0) = 0, f'(0) = 1, f'(\infty) &\to 0 \\ \theta'(0) = -\gamma_1(1-\theta(0)), \theta(\infty) &\to 0 \\ \phi'(0) = -\gamma_2(1-\phi(0)), \theta(\infty) &\to 0 \end{aligned} \tag{16}$$

with viscosity ratio constant $\beta_1 = \frac{\mu_\infty}{\mu_0}$, Weissenberg parameter $We = \Gamma\sqrt{\frac{a^3x^2}{v}}$, Prandt1 number $\Pr = \frac{v}{\alpha_{nf}}$, Schmidt number $\mathrm{Sc} = \frac{v}{D_B}$, thermophoresis parameter $Nt = \tau D_T\left(T_f - T_\infty\right)/T_\infty$ ν Brownian movement parameter $Nb = \tau D_B\left(C_f - C_\infty\right)/\nu C_0$, thermal Biot number $\gamma_1 = \frac{h_f}{k}\sqrt{\frac{v}{a}}$, mass Biot number $\gamma_2 = \frac{h_g}{D}\sqrt{\frac{V}{a}}$, mixed convective parameter $\lambda^* = \frac{xg\gamma_1(T_f - T_\infty)}{a^2x^2}$, buoyancy ratio $\Omega_1 = \frac{\beta_C(C_f - C_\infty)}{\beta_T(T_f - T_\infty)}$ and Hartmann number $Ha = \sqrt{\frac{\sigma B_0^2}{\rho a}}$. The wall shear force is for Carreau nanofluid flow is given by [23,24]:

$$C_f = \frac{\tau_w}{\rho u_s^2}, \tau_w = \mu_0\left(\frac{\partial u}{\partial y}\right)\left[\beta_1 + (1-\beta_1)\left\{1 + \Gamma^2\left(\frac{\partial u}{\partial y}\right)\right\}^2\right\}^{\frac{n-1}{2}}\Bigg]_{y=0} \tag{17}$$

which is in dimensionless form

$$\mathrm{Re}_x^{1/2} C_f = \beta_1 f''(0) + (1-\beta_1) f''(0)\left(1 + (We)^2\left(f''(0)\right)^2\right)^{\frac{n-1}{2}} \tag{18}$$

The equations for local Nusselt number and local Sherwood number are [23, 24]:

$$\begin{aligned} Nu_x &= \frac{xq_h}{k\left(T_f - T_\infty\right)} \\ Sh_x &= \frac{xq_s}{D_B\left(C_f - C_\infty\right)} \end{aligned} \tag{19}$$

In dimensionless form

$$\begin{aligned} \frac{Nu}{\sqrt{\mathrm{Re}_x}} &= -\theta'(0) \\ \frac{Sh}{\sqrt{\mathrm{Re}_x}} &= -\phi'(0) \end{aligned} \tag{20}$$

§3 Modeling of entropy generation

Entropy generation in presence of viscous dissipation irreversibility, heat transfer irreversibility, mass transfer irreversibility and Joule heating irreversibility is expressed as [13-16]:

$$S_G = \frac{\mu}{T_\infty}\left[\beta_1 + (1-\beta_)\left\{1 + \Gamma^2\left(\frac{\partial u}{\partial y}\right)^2\right\}^{\frac{n-1}{2}}\right]\left(\frac{\partial u}{\partial y}\right)^2 + \frac{\sigma B_0^2}{T_\infty}u^2 + \frac{k}{T_\infty^2}\left(\frac{\partial T}{\partial y}\right)^2 + \tag{21}$$

$$R^* D \left(\frac{1}{C_\infty} \frac{\partial C}{\partial y} + \frac{1}{T_\infty} \frac{\partial T}{\partial y} \right) \frac{\partial C}{\partial y}. \tag{22}$$

After implementation of transformation dimensionless form of equation is presented as:

$$N_G = B_r \left(f''\right)^2 \left[\beta_1 + (1-\beta_1) \left(1 + \frac{n-1}{2} (We)^2 \left(f''\right)^2 \right) \right] + M^2 B_r \left(f'\right)^2 + \alpha_1 \theta'^2 + R^* \frac{\alpha_1^*}{\alpha_1} \phi'^2 + R^* \theta' \phi'. \tag{23}$$

Bejan number is the ratio of heat and mass transfer irreversibility to total entropy. Mathematical expression is addressed as [13-16]:

$$B_e = \frac{\alpha_1 \theta'^2 + R^* \frac{\alpha_1^*}{\alpha_1} \phi'^2 + R^* \theta' \phi'}{B_r \left(f''\right)^2 \left[\beta_1 + (1-\beta_1) \left(1 + \frac{n-1}{2} (We)^2 \left(f''\right)^2 \right) \right] + M^2 B_r f'^2} \alpha_1 \theta'^2 + R^* \frac{\alpha_1^*}{\alpha_1} \phi'^2 + R^* \theta' \phi'. \tag{24}$$

§4 Discussion

This section deals with the physical interpretation of Figs. (1-15) and Tables (1-3). In these Figures and Tables trends of velocity, temperature, concentration, Bejan number, entropy generation, skin friction, Sherwood number and Nusselt number against different important parameters is shown. While varying each parameter, remaining parameters kept fixed values like $\beta_1 = 0.5,\ We = 0.2,\ \Pr = 0.2,\ Nt = 0.4,\ Nb = 0.2,\ \gamma_1 = 0.1,\ \gamma_2 = 0.2,\ \lambda^* = 0.5,\ \Omega_1 = 0.3,\ Ha = 0.2$.

Figs. (1-3) are designed to show the impact of viscosity ratio parameter β, Weissenberg number We and Hartman number M on velocity field. It is seen that velocity of the fluid enhances for higher values of β_1. It is due to the fact that zero viscosity shear rate decays with higher values of $\beta_1 = 0.2, 0.4, 0.6, 0.8$ hence resistance between the fluid particles reduces consequently velocity enhances. Fig. 2 expresses the impact of Weissenberg number on velocity profile. Motion of the fluid slows down with higher estimation of We. Physically with enhancement of We relaxation time enhances due to which resistances also increases consequently velocity of the fluid decays. It is worth remarking that the observation illustrated as Fig. 2 corroborates with one of the comes by Abegunrin [27] in a study on comparison between the flow of Williamson to Casson fluid. Both observations are justifiable because such decrement can be traced to the fact that shear stress profile definitely decreases negligible within the fluid domain. Fig. 3 delineates the influence of magnetic parameter M on velocity field. It is shown that velocity decreases with increase in M. When we increase the values of M Lorentz force also enhances which is responsible for decrease in velocity.

Figs. $(4-6)$ are designed to show the impact of different parameters on temperature profile. Fig. 4 shows the impact of thermophoresis parameter Nt on temperature. It is noticed that temperature of the fluid is higher for greater values of Nt. Temperature difference rises with increase in Nt due to which particles move from hotter region to colder region and temperature enhances. Impact of Biot number on temperature profile is shown in Fig. 5. When we increase

the values of Biot number heat transfer coefficient rises hence temperature enhances. Fig. 6 deals with the influence of Brownian motion parameter against temperature field. It is seen that temperature is increasing function of Nb. Random motion of nanofluids particles started due to which temperature of the fluid boosts up.

Figs. (7-9) elaborate the impact of different parameters on concentration field. It is seen that concentration profile rises for greater values of solutal Biot number. Mass transfer coefficient increases for higher Biot number owing to which concentration enhances. Fig. 8 describes the behavior of Schmidt number Sc against concentration profile. Sc is the ratio of momentum to mass diffusivity. Decrement in mass diffusivity occurs with increase in Sc hence concentration profile decays. Increase in concentration profile is noticed for higher values of Nt (See Fig. 9). Figs. (10-15) explain the effect of involved parameters on entropy generation and Bejan number. Figs. (10 and 11) describes the impact of Brinkman number Br on entropy generation and Bejan number Be. With increase in values of Br entropy generation boosts up. When we increase the values of Br viscosity of the fluid enhances. Increase in viscosity enhances the viscous dissipation irreversibility due to which entropy of the fluid rises (See Fig. 10). Fig. 11 shows that Bejan number decays for higher estimation of Br. When Br = 0 Bejan number attain its maximum value. Figs. 12 and 13 show the impact of diffusion parameter on entropy generation and Bejan number. It is observed that irreversibility of the fluid enhances due to increase in mass transfer irreversibility. Fig. 13 depicts that Bejan number is increasing function of diffusion parameter because mass transfer irreversibility is dominant over viscous dissipation irreversibility. Figs. (14 and 15) tell the effect of Biot number on entropy generation and Bejan number. It is noticed that entropy of the fluid decays via increasing values of Biot number. While Bejan number reduces near the sheet and then starts increasing for higher values of Biot number.

Tables (1-3) describe the effect of different involved parameters against skin friction, Nusselt number and Sherwood number. Surface drag force enhances for higher values of Weissenberg number We, viscosity ratio parameter β and mixed convection parameter λ^* while skin friction rises for higher values of n (See Table 1). Table 2 describes that heat transfer enhances for higher values of Pr and Ec While opposite impact is depicted for higher Nt and Nb. Table 3 tells the influence of Sherwood number against Schmidt number Sc, thermophoresis parameter Nt and Brownian motion parameter Nb. Sherwood number is increasing function of Sc and Nb while opposite behavior is seen for Nt. In a recent meta-analysis on the transport phenomenon of various nanofluids, it was concluded that increasing haphazard motion of tiny/nano-sized particles is capable to cause an increase in the internal pressure on the tiny particles.

§5 Conclusion

Here we consider the Carreau nanofluid MHD flow with viscous dissipation effect. Entropy generation and Bejan number for Carreau nanofluid are also analyzed in detail. Main points are presented below:

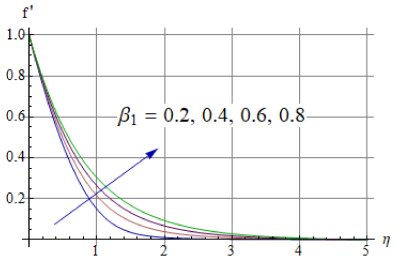

Fig 1. Velocity field versus β.

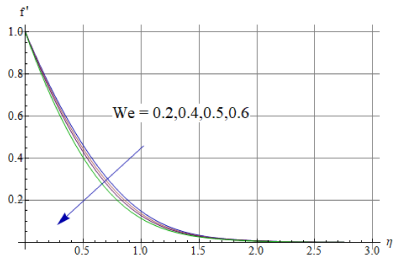

Fig 2. Velocity field versus We.

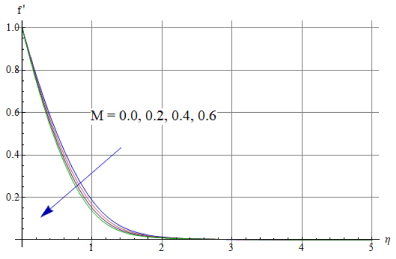

Fig 3. Velocity field versus M.

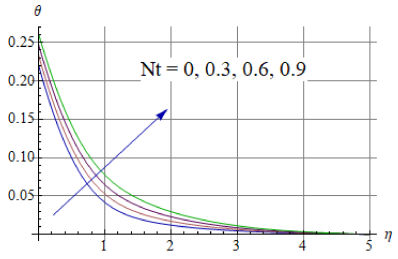

Fig 4. Temperature field versus Nt.

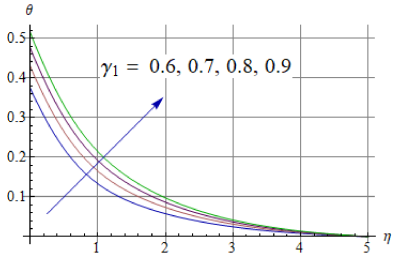

Fig 5. Temperature field versus γ_1.

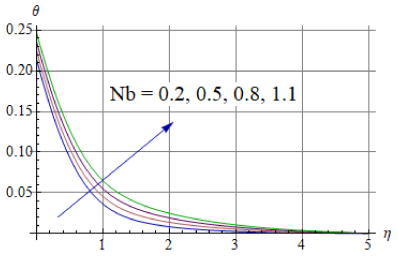

Fig 6. Temperature field versus Nb.

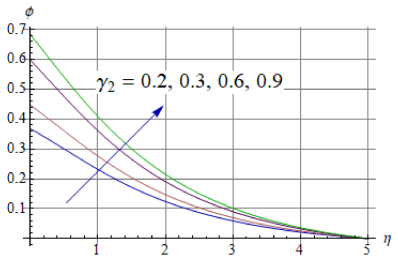

Fig 7. Concentration field versus γ_2.

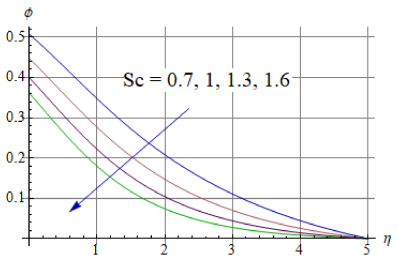

Fig 8. Concentration field versus Sc.

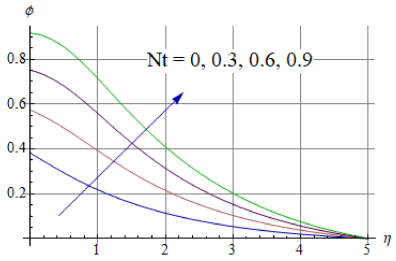

Fig 9. Concentration field versus Nt.

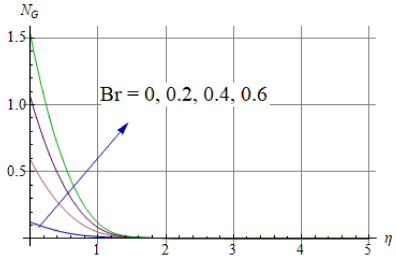

Fig 10. Entropy generation versus Br.

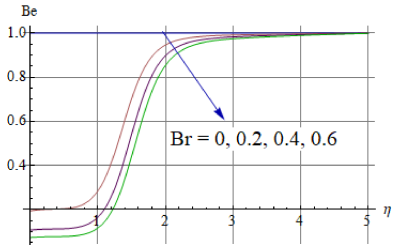

Fig 11. Bejan number versus Br.

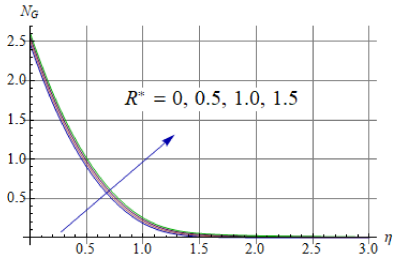

Fig 12. Entropy generation versus R^*.

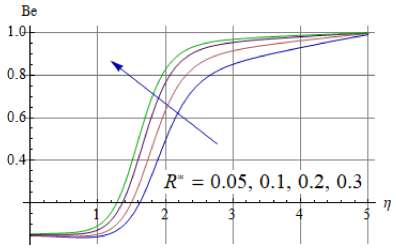

Fig 13. Bejan number versus R^*.

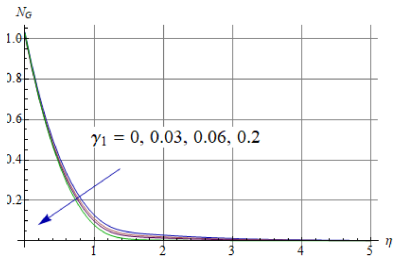

Fig 14. Entropy generation versus γ_1.

Table 1. Skin friction for different values of We, n, β_1 and λ^*.

We	n	β_1	λ^*	Skin friction
0.2	0.3	0.2	0.2	-1.27773
0.3				-1.26964
0.4				-1.26363
0.2	0.4			-1.27946
	0.5			-1.28118
	0.3	0.3		-1.26136
		0.4		-1.24476
		0.2	0.3	-1.27109
			0.4	-1.2645

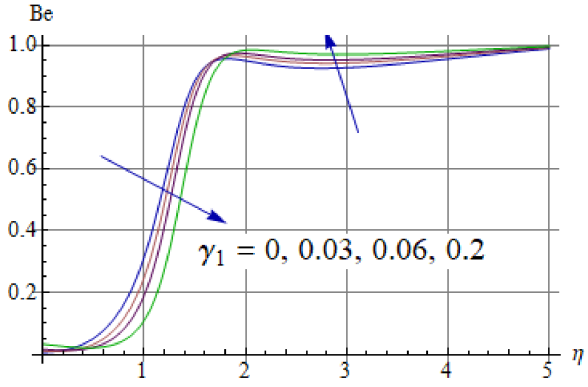

Fig 15. Bejan number versus γ_1.

Table 2. Nusselt number for different values of Pr, Nt, Nb and Ec.

Pr	Nt	Nb	Ec	Nusselt number
1.2	0.1	0.5	0.4	0.332483
1.3				0.342614
1.4				0.352112
1.2	0.2			0.330604
	0.3			0.328688
	0.1	0.6		0.33101
		0.7		0.329512
		0.5	0.5	0.361643
			0.6	0.391406

- Velocity of the fluid decays for higher values of We and M.
- The temperature rises for Nt and Nb which are the main parameters of nanofluid based on the Buongiorno nanofluid model.
- Temperature rises for Nt and Nb.
- Concentration profile decays for larger Sc and enhances for greater Solutal Biot number and Nt.
- Entropy generation is increasing for Brinkman number and diffusion parameter.
- Bejan number is maximum (Be = 1) for Br = 0.
- Skin friction enhances for Weissenberg number and mixed convection parameter.
- Heat transfer is larger for Pr and Ec.
- Mass transfer is highest for larger values of Sc and Nb.

Table 3. Sherwood number for different values of Sc, Nt and Nb.

Sc	Nt	Nb	Sherwood number
1	0.1	0.5	0.162692
1.1			0.167972
1.2			0.172867
1	0.2		0.141236
	0.3		0.120256
	0.1	0.6	0.166508
		0.7	0.169247

Declarations

Conflict of interest The authors declare no conflict of interest.

References

[1] S U S Choi. *Enhancing thermal conductivity of fluids with nanoparticles*, Int Mech Eng Cong Exp, ASME, FED 231/ MD, 1995, 66: 99-105.

[2] J Buongiorno. *Convective transport in nanofluids*, J Heat Transfer, 2006, 128(3): 240-250.

[3] M Turkyilmazoglu. *Fully developed slip flow in a concentric annuli via single and dual phase nanofluids models*, Comput Meth Prog Biomed, 2019, 179: 104997.

[4] B Souayeh, K G Kumar, M G Reddy, S Rani, N Hdhiri, H Alfannakh, M Rahimi-Gorji. *Slip flow and radiative heat transfer behavior of Titanium alloy and ferromagnetic nanoparticles along with suspension of dusty fluid*, J Mol Liq, 2019, 290: 111223.

[5] A Wakif, I L Animasaun, P V S Narayana, G Sarojamma. *Meta-analysis on thermo-migration of tiny/nano-sized particles in the motion of various fluids*, Chin J Phys, 2020, 68: 293-307.

[6] A Hajizadeh, N A Shah, S I A Shah, I L Animasaun, M Rahimi-Gorji, I M Alarifi. *Free convection flow of nanofluids between two vertical plates with damped thermal flux*, J Mol Liq, 2019, 289: 110964.

[7] Z Nisar, T Hayat, A Alsaedi, B Ahmad. *Significance of activation energy in radiative peristaltic transport of Eyring-Powell nanofluid*, Int Commun Heat Mass Transf, 2020, 116: 104655.

[8] I Mustafa, A Ghaffari, T Javed, J N Abbasi. *Numerical examination of thermophysical properties of Cobalt Ferroparticles over a wavy surface saturated in non-Darcian porous medium*, J Non-Equilib Thermodyn, 2020, 45(2): 109-120.

[9] Y M Chu, F Ahmad, M I Khan, M Nazeer, F Hussain, N B Khan, S Kadry, L Mei. *Numerical and scale analysis of non-Newtonian fluid (Eyring-Powell) through pseudo-spectral collocation method (PSCM) towards a magnetized stretchable Riga surface*, Alex Eng J, 2021, 60(2): 2127-2137.

[10] Y M Chu, S Aziz, M I Khan, S U Khan, M Nazeer, I Ahmed, I Tlili. *Nonlinear radiative bioconvection flow of Maxwell nanofluid configured by bidirectional oscillatory moving surface with heat generation phenomenon*, Phys Scripta, 2020, 95(10): 105007.

[11] M Kumar, K P Kashyap, N N Kumar. *Effect of magnetite nanoparticles on couple stress fluid between two parallel squeezing and expanding surfaces*, SN Appl Sci, 2020, 2: 848.

[12] A S Oke, I L Animasaun, W N Mutuku, M Kimathi, N A Shah, S Saleem. *Significance of Coriolis force, volume fraction, and heat source/sink on the dynamics of water conveying 47 nm alumina nanoparticles over a uniform surface*, Chinese J Phys, 2021, https://doi.org/10.1016/j.cjph.2021.02.005.

[13] M Kumar, G J Reddy, N Dalir. *Transient entropy analysis of the magnetohydrodynamics flow of a Jeffrey fluid past an isothermal vertical flat plate*, Pramana, 2018, 60: 91.

[14] N Shukla, P Rana, O A Bg. *Unsteady MHD non-Newtonian heat transfer nanofluids with entropy generation analysis*, Nonlinear Eng, 2019, 8: 630-644.

[15] M R Salimi, M Taeibi-Rahni, H Rostamzadeh. *Heat transfer and entropy generation analysis in a three-dimensional impinging jet porous heat sink under local thermal non-equilibrium condition*, Int J Thermal Sci, 2020, 153: 106348.

[16] M Khan, A Shahid, M ElShafey, T Salahuddin, F Khan. *Predicting entropy generation in flow of non-Newtonian flow due to a stretching sheet with chemically reactive species*, Comput Meth Prog Biomed, 2020, 187: 105246.

[17] Y M Chu, F Shah, M I Khan, S Kadry, Z Abdelmalek, W A Khan. *Cattaneo-Christov double diffusions (CCDD) in entropy optimized magnetized second grade nanofluid with variable thermal conductivity and mass diffusivity*, J Mater Resear Techn, 2020, 9(6): 13977-13987.

[18] N Khan, I Riaz, M S Hashmi, S A Musmar, S U Khan, Z Abdelmalek, I Tlili. *Aspects of chemical entropy generation in flow of Casson nanofluid between radiative stretching disks*, Entropy, 2020, 22(5): 495.

[19] S M Seyyedi, A S Dogonchi, M H Tilehnoee, M Waqas, D D Ganji. *Entropy generation and economic analyses in a nanofluid filled L-shaped enclosure subjected to an oriented magnetic field*, Appl Thermal Eng, 2020, 168: 114789.

[20] M Kumar, G J Reddy, G R Kiran, M A M Aslam, O A Beg. *Computation of entropy generation in dissipative transient natural convective viscoelastic flow*, Heat Transfer Asian Resear, 2019, 48(3): 1067-1092.

[21] O K Koriko, K S Adegbie, N A Shah, I L Animasaun, M A Olotu. *Numerical solutions of the partial differential equations for investigating the significance of partial slip due to lateral velocity and viscous dissipation: The case of blood-gold Carreau nanofluid and dusty fluid*, Numer Meth Partial Diff Eq, 2021, https://doi.org/10.1002/num.22754.

[22] P J Carreau. *Rheological equations from molecular network theories*, Trans Soc Rheol, 1972, 16: 99-127.

[23] T Hayat, S Qayyum, M Waqas, B Ahmed. *Influence of thermal radiation and chemical reaction in mixed convection stagnation point flow of Carreau fluid*, Results Phys, 2017, 7: 4058-4064.

[24] M Khan, M Y Malik, T Salahuddin. *Heat generation and solar radiation effects on Carreau nanofluid over a stretching sheet with variable thickness: Using coefficients improved by cash and carp*, Results Phys, 2017, 7: 2512-2519.

[25] M Farooq, Q A Anzar, T Hayat, M I Khan, A Anjum. *Local similar solution of MHD stagnation point flow in Carreau fluid over a non-linear stretched surface with double stratified medium*, Results Phys, 2017, 7: 3078-3089.

[26] I L Animasaun, R O Ibraheem, B Mahanthesh, H A Babatunde. *A meta-analysis on the effects of haphazard motion of tiny/nano-sized particles on the dynamics and other physical properties of some fluids*, Chinese J Phys, 2019, 60: 676-687.

[27] O A Abegunrin, S O Okhuevbie, I L Animasaun. *Comparison between the flow of two non-Newtonian fluids over an upper horizontal surface of paraboloid of revolution: Boundary layer analysis*, Alex Eng J, 2016, 55(3): 1915-1929.

[1]School of Science, Hunan City University, Yiyang 413000, China.
[2]Department of Mechanical Engineering, Prince Mohammad Bin Fahd University, P. O. Box, 1664, Al-Khobar 31952, Kingdom of Saudi Arabia.
[3]Department of Mathematics, Namal University, Mianwali 42250, Pakistan.
[4]Department of Mathematics, Quaid-I-Azam University 45320, Islamabad 44000, Pakistan.
Email: mikhan@math.qau.edu.pk